Regulation of Solid-state Dual-emission Properties by Switching Luminescent Processes Based on the Bis-*o*-carborane-modified Anthracene Triad

Kazuhiro Yuhara, Kazuo Tanaka* and Yoshiki Chujo

Department of Polymer Chemistry, Graduate School of Engineering, Kyoto University

Katsura, Nishikyo-ku, Kyoto 615-8510, Japan

E-mail: tanaka@poly.synchem.kyoto-u.ac.jp

Abstract

We herein demonstrate not only design of combination of luminescent processes in dual-emission properties by selecting preparation protocols but also temperature-driven switching of luminescent processes in dual-emission properties based on the bis-*o*-carborane-substituted anthracene triad in crystal. We synthesized the triad and obtained crystal polymorphs with or without solvent molecules by changing the type of solvent in recrystallization. From the optical measurements, it was shown that dual emission properties are composed of different photophysical mechanisms. That is, In the absence of the solvent molecules the crystal exhibits dual emission of charge transfer (CT) and excimer, while in the presence of them the crystal exhibits that of locally-excited (LE) and CT emission. Furthermore, intensity ratios between them were sensitive to temperature changes. These luminochromic behaviors are suitable for the application to ratiometric sensing systems.

Introduction

The dual emission system, in which two emission bands are simultaneously observed in the spectra, is a versatile optical behavior.[1] For example, to obtain white luminescence, dual emission is necessary with appropriate color balance.[2] Generally, by loading several dyes having different luminescent color onto matrices, desired luminescent color is generated. As another instance, if intensity ratios among emission components are varied by environmental changes, precise detection for the changes can be realized through ratiometric analyses.[3] By comparing emission intensities at various wavelength positions, we can exclude influence from the heterogeneity of local concentration of luminophores on the signals. This function is of importance especially for realizing quantitative analyses.[4] Therefore, it can be said that design and synthesis of dual emission systems should be of significance for developing advanced luminescent materials and sensors.

In the solution system, several approaches have been established for obtaining dual emission. By suppressing transition in the excited state between locally-excited (LE) and charge-transfer (CT) states, dual emission has been often achieved.[5] Owing to high environmental sensitivity of excited molecules, dual-emissive materials can be utilized as a key component for optical chemical sensors.[6] The dual emission consisting of LE and excimer emission has been also accomplished.[7] Drastic color changes can be obtained because of intrinsic intense emission from excimer. Additionally, by

connecting different types of molecules and suppressing energy transfer efficiency, dual emission can be produced.[8] Clear color changes according to the preprogrammed design are often observed. In particular, for naked eyes, dual emission is advantageous for enhancing visibility because of apparent drastic color changes.[9] Even if environmental factors are slight, drastic emission color changes can be observed.[10] Thus, dual emission properties are suitable for designing luminescent sensors. However, there are still difficulties in the design of dual emission systems in the solid state. Most of luminescent properties are generally spoiled by non-specific intermolecular interactions in the condensed state. Moreover, due to structural restriction, it is challenging to design luminochromic behaviors based on dual emission properties. Although several unique materials have been recently discovered, robust design strategies are still explored for observing dual emission in solid.

o-Carborane (1,2-dicarba-*closo*-dodecarborane) is an icosahedral cluster composed of ten boron, two carbon and hydrogen atoms on each vertex. The bulky and sphere structure of *o*-carborane is often useful for avoiding concentration quenching, followed by inducing intense solid-state emission.[11–14] Various solid-state luminochromic behaviors were observed from aryl-substituted *o*-caboranes such as anthracene,[15] pyrene[16] and 1,4-bis(phenylethynyl)benzene.[17] Moreover, *o*-carborane derivatives with dual emission properties have been discovered. Therefore, we have also

paid tremendous attention to aryl-modified *o*-carboranes as a platform for obtaining functional solid-state luminescent materials. From the first report on aggregation-induced emission of *o*-carborane-containing polymers,[18] the series of stimuli-responsive luminescent materials have been developed.[19] More recently, environmental sensing has been accomplished by the combination with luminochromic properties as well as intensity changing ability.[20] Thus, we regard *o*-carborane as a solid-state luminescent chromism-inducible "element block," which is the minimum functional building block including hetero atoms.[21–24] According to the mechanistic studies on environment-sensitive luminescent properties, it was revealed that molecular rotation in the *o*-carborane unit in the condensed state is allowed, and various luminescent color can be expressed by regulating the angle between the direction of the C–C bond in *o*-carborane and π-plane.[25,26] In the planar and vertical conformation between them, LE and CT emission can be respectively induced even in the solid state. On the basis of these structure-relating optical properties, stimuli-responsive luminochromic behaviors have been observed from the solid materials by regulating degree of molecular rotation.[27] Additionally, solid-state excimer emission from ethynylacridine-modified *o*-caborane was recently reported.[28] Weakly-acidic hydrogen on the unsubstituted carbon atom in *o*-carborane plays an important role in the formation of dimer in the crystalline state, followed by excimer.[29] It should be noted that these materials showed clear thermochromic behaviors originating from mechanism switch from excimer to CT emission.[30] Moreover, by introducing the

bis-*o*-carborane substituents, highly-sensitive luminochromic behaviors were observed.[31,32] Bis-*o*-carborane-substituted pyrene triad showed clear luminochromic behaviors just by touching the crystalline powder.[32] Because of steric hindrances of *o*-carboranes, defect sites in crystalline packing could be readily induced by weak stimuli. As a result, CT emission was converted to excimer emission, followed by luminochromism, triggered by such tiny external stimuli. Thus, we presumed that introduction of multiple *o*-carborane substituents could be a promising strategy for obtaining diverse solid-state luminochromic behaviors as well as highly-sensitive stimuli-responsiveness.

Herein, synthesis and optical properties of bis-*o*-carborane-modified anthracene triad **1** are reported (Figure 1). We were able to obtain crystal polymorphs with or without solvent molecules by changing the solvent type in recrystallization and found that each polymorph provides characteristic solid-state dual emission behaviors. In the absence of solvent molecules, dual emission consisting of CT and excimer emission was detected, while dual emission composed of LE and CT emission was observed in the presence of solvent molecules. Remarkably, both crystals showed thermochromic luminescence based on intensity ratio changes between dual emission bands. These behaviors are advantageous for precisely estimating temperature through ratiometric analyses with dual emission properties of **1**. This is the first example, to the best of our knowledge, to offer temperature-driven switching of luminescent processes in dual-emission properties in crystal as well as design of

combination of luminescent processes in dual-emission properties by selecting preparation protocols.

Figure 1

Results and Discussion

Molecular design and synthesis

As mentioned in the introduction, the modified aromatics having multiple *o*-carborane substituents is a promising platform for realizing stimuli-responsive dual emission in the solid state. So far, dual emission with thermochromic properties was achieved by controlling LE and CT emissions of aryl-modified *o*-carborane dyads by regulating the angle between the π-plane of the aryl moiety and the C–C bond in the *o*-carborane unit.[33] Furthermore, by modulating energy barrier of molecular rotation, thermochromic luminescence was accomplished.[34] On the other hand, regulation of the dual emission behavior concerning excimer is still challenging. On the basis of solid-state dual-emission properties of *o*-carboranes consisting of LE and CT emission, we sought to additionally combine excimer emission as another luminescent species. Excimer emission has relatively longer lifetime than fluorescence and appears as a distinct emission band at the medium position between LE and CT emission bands. To achieve dual emission involving excimer emission, we designed the bis-*o*-carborane-substituted anthracene triad **1**. Anthracene is known as a typical aromatic ring with luminescent properties and has been employed as an aryl moiety for constructing *o*-carborane dyads because of its efficient absorption and emission properties.[35] Similarly to the previous solid-state aryl-modified *o*-carborane dyads presenting LE and CT emission because of steric hindrances and spatial repulsion of the sphere cluster structure, *o*-carboranes are directly connected to the aryl

moiety.[16,25,36,37] In the previous works, we introduced *o*-carborane units only to the center benzene ring of the three rings in anthracene such as 9- or 10-positions. This strategy induced the dual-emission properties between LE and CT emission, while it resulted in absence of the π–π interaction of the anthracene moieties attributed to the curved structure of the anthracene rings like butterfly and the large steric hindrance of the carborane units.[11,15,25] In particular, by placing *o*-carboranes at the both sides of the anthracene's three benzene rings such as 1 and 8 positions to reduce the distortion of the anthracene units, we presumed that intermolecular interaction between anthracenes, which is essential for forming excimer, might be capable (Figure 1). As a result, solid-state excimer emission can be obtained in the solid state with LE or CT emission. To validate this idea, we introduced *o*-carborane units to 1,8-positions of anthracene.

The triad **1** was synthesized by the alkyne insertion reaction with decaborane and 1,8-diethynylanthracence (Scheme S1).[38] The product was obtained by silica-gel column chromatography followed by recrystallization. The chemical structure of the product was unambiguously characterized by ^{1}H, ^{11}B and ^{13}C{^{1}H} NMR spectroscopy, high-resolution mass spectroscopy, single-crystal X-ray and elemental analyses (Charts S1–S3).

Polymorphism

By changing the type of solvents for recrystallization, we were able to obtain polymorphs with

different optical properties as well as crystal packing. When **1** was recrystallized from CCl_4, the yellow crystal (**1a**) was obtained, while from toluene, $CHCl_3$ and cyclohexane, the light-yellow crystals (**1b**–**1d**) was obtained, respectively (Figure S1). From ^{1}H NMR spectroscopy and thermogravimetric analyses, **1a** has no solvent molecules, whereas **1b**–**1d** included 0.5 equivalent of solvent molecules during recrystallization (Charts S4–S7, Figure S2 and Tables S1 and S2). From the powder X-ray diffraction (PXRD) data, two crystals had diffraction peaks at different positions (Figure S3). Based on these results, we concluded that **1** has crystal pseudo-polymorphs depending on the recrystallization solvents. Additionally, we found that transition from **1b**–**1d** to **1a** can be proceeded by heating. When **1b**–**1d** were heated at 200 °C for 5 min, the transformation to **1a** with the clear color change from light yellow to yellow occurred. In the profile of differential scanning calorimetry with **1b**, the endothermic peak was observed at 156 °C, corresponded to the desorption of included solvents (Figure S5). Similar profiles were obtained from **1c** and **1d**. PXRD patterns of the heated **1b**–**1d** were identical to **1a** (Figure S3). ^{1}H NMR spectra of those samples also indicated that no solvent molecules should be included in each crystal after heating (Charts S8–S11). Furthermore, transformations from **1a** to **1b–1d** were investigated (Figure S4). When **1a** was exposed to the solvent vapors such as toluene, $CHCl_3$ and cyclohexane, PXRD patterns and color didn't changed. In contrast, when **1a** was immersed to toluene, clear color changes from yellow to light yellow were detected. PXRD pattern was almost same as **1b**. Therefore, it was revealed that the

immersing to toluene is one of the solvent including strategies to **1a** other than recrystallization. These results suggest that the crystal polymorphism of **1**, followed by optical properties, can be controlled by choosing recrystallization solvents and heating.

To obtain insight on the crystal packings, single-crystal X-ray structures were analyzed. From **1b**, the suitable sample for the analysis was fortunately obtained through slow evaporation from toluene (Figure 2 and Table S4 and S5). **1b** included 0.5 equivalent of toluene as mentioned above, although the disordered solvent molecules were removed during the analysis by the SQUEEZE method.[39] According to the result, it was found that **1b** has the monoclinic $P2_1/c$ space group, and intermolecular π–π interaction between anthracene rings was not observed. It is because the twisted anthracene rings ($\varphi_{C1\text{-}C4\text{-}C5\text{-}C8}$ = 22.0(1)°) should disturb interaction. We assumed that the twisted anthracene ring in **1b** might be formed by bulky *o*-carborane units and this distorted conformation could be stabilized by included solvents. The X-ray analysis of **1a** was performed, but the *R* value was too large to discuss detailed structural properties (Figure S6 and Table S3). Since the crystal packing was able to be decided only from **1b** and similar optical properties were obtained from **1b**–**1d** (Figure S8 and S12 and Table S14), we mainly discuss differences in optical properties between **1a** and **1b**.

Photophysical Properties

Photophysical properties of **1** were investigated. Initially, to evaluate the electronic structure of **1**, optical measurements were performed with the diluted solution (Figure 3 and Table 1). Absorption spectra of **1** had vibrational structures attributed to the π–π* transition at the anthracene moiety (Figure 3a). Comparing to anthracene, the slight red shift of the absorption band from the modified anthracene can be explained by the electron-withdrawing effect of *o*-carborane.[40] Because of electron-deficiency of the *o*-carborane substituents, significant electronic communication should be formed, followed by stabilization of energy levels. Consequently, the bathochromic peak shift should proceed. The data from TD-DFT calculations revealed that electronic conjugation is expanding to the *o*-carborane unit, supporting this speculation (Figure S7 and Tables S6–S13). To estimate electronic structure of **1** in the excited state, photoluminescence (PL) properties were examined. Accordingly, obvious two emission bands were detected (Figure 3a). Since the bathochromic shift was observed only from the emission band in the longer wavelength region in polar solvents, we concluded that the emission band with vibrational structure in shorter wavelength region and the broad band in the longer one should be attributable to the emission originating from the transition from the locally-excited (LE) state at the anthracene moiety and from the intramolecular charge transfer (CT) state involving a whole molecule, respectively (Figures S13–S15 and Table S15).

Next, solid-state optical properties of **1** were investigated (Figure 3b and Table 1). The obtained data of **1c** and **1d** were almost the same as those of **1b** (Figure S8 and S12 and Table S14). Thus, we

discuss solid-state optical properties of **1** with the data of **1b**. Diffusion reflectance spectra revealed that the offset wavelength of **1a** was about 50 nm longer than those of **1b** (Figure 3b). This result suggests that π–π overlapping of the anthracene rings should exist in the crystalline structure of **1a**. In the PL spectra, **1a** showed the far broader emission band, whereas **1b** exhibited similar unimodal emission bands with the peaks around 608 nm (Figure 3b). Not only crystal packing but also molecular conformation should be greatly influenced by included solvents. To gain deep insight on the emission mechanism, we performed PL lifetime measurements (Figures S10 and S11 and Table S14). **1a** had relatively longer lifetime component (53 ns) and shorter component (10 ns), while **1b** mainly had relative shorter components (11 ns) (Table 1). Furthermore, when **1** was dispersed in polystyrene with a concentration of 1 wt%, the emission band with the shorter lifetime was observed in almost the same wavelength region to the crystalline sample (Figures S16 and S17 and Table S16). Since each molecule should be isolated in the polystyrene matrix, the emission band in the longer wavelength region with the shorter lifetime is attributable to CT emission.

It should be noted that spectrum shape alteration was observed from the crystalline sample of **1a** by delaying detection time. The emission spectrum of **1a** converged into a unimodal band in the shorter wavelength region after 30 ns, meanwhile a significant shape change was hardly observed from the spectrum of **1b** even after 50 ns (Figure S18). This fact implies that the different emission species from CT emission might be generated in the crystalline sample of **1a**. As mentioned above, **1**

showed only CT emission in the polystyrene matrix, where intermolecular interaction would be negligible, and basically, the longer lifetime than those from conventional fluorescence was observed from **1a**. From these data, we concluded that the converged emission band should be attributable to excimer emission from the anthracene moieties. In summary, **1** can exhibit three types of emission bands: LE, CT and excimer emission, and the latter two processes are dominant in solid. In particular, intensity ratios of CT and excimer emission are critically dependent on environmental factors, such as distribution in crystal packing and the vicinity of solvent molecules and can be varied by employing polymorphs. In addition, in the absence of solvent molecules, dual emission and the time-course change in emission ratios between CT and excimer emission were observed. In the presence of solvent molecules, only CT emission was observed.

Thermochromic Luminescence

Finally, we examined stimuli-responsivity of dual emission of **1** in the crystalline state. Characteristic thermochromic luminescence behaviors were observed from the crystalline samples of **1** in the wide temperature range between 80 K and 440 K (Figures 4, S19–S21). Below 200 K, **1a** showed the broad and unimodal emission band, while in the case of **1b**, additional emission band with vibrational structures in the shorter wavelength regions was also detected. This emission band is attributable to LE emission. It is like that the planar conformation of the C–C bonds in *o*-carborane

units and π plane, which is suitable for providing LE emission, should be maintained by suppressing molecular rotation at the *o*-carborane unit in the low temperature region. Different behaviors were also obtained over 200 K. **1a** continuously exhibited the unimodal broad emission band with the peak around 570 nm (Figure 4a). Subsequently, by heating, this emission band hypsochromically shifted, and as we expected, dual emission involving the new band around 640 nm was observed. Taking into consideration of the peak positions of these emission bands, the former and latter emission could be assigned as excimer and CT emission, respectively. In contrast, the broad emission band in the longer wavelength region exhibited bathochromic shift in **1b** (Figure 4b). Judging from the peak position, this emission band is attributable to CT emission. We previously reported the same results of emission band shifts upon heating.[11,29] From excimer emission, hypsochromic shifts were observed, and it was suggested that intermolecular interaction through π–π stacking should be weakened by the gradual expansion of crystal lattice. In contrast, bathochromic shifts were detected from CT emission and it was proposed that larger structural relaxation could be allowed in weakened crystal packing where thermal motions at the substituents vigorously occur. Owing to such opposite tendency in the peak shift between excimer and CT emission by heating, sensitive thermochromic responsibility was achieved. In the case of **1a**, as temperature increased, excimer/CT intensity ratio increased. It is probably because gradual expansion of the distance of π–π stacking lead to more favorable conformation for CT emission than for excimer emission. In the case

of **1b**, intensity of LE emission was lowered by heating, and bathochromic shift of the CT emission band was simultaneously observed. It is reasonable that molecular rotations should be enhanced, followed by enhancement of CT emission. When thermochromic luminescence of **1a** was monitored by cooling from 440 K to 80 K, followed by heating from 80 K to 440 K, almost same spectra were obtained (Figure S21). Therefore, the reversibility of this thermochromic luminescence was confirmed. After heating **1b** at 440 K, we cooled the crystalline sample to 80 K and monitored luminescent properties by 2nd heating. Accordingly, the same behavior to **1a** was obtained (Figures S19 and S20). Because of desorption of solvent molecules by heating, **1a** was generated without significant pyrolysis and switching of the dual emission property consisting of LE and CT emission of **1b** to that of excimer and CT emission of **1a** can be realized.

Conclusion

Solid-state thermochromic luminescence of bis-*o*-carborane-modified anthracene triad **1** is reported. In the several previous reports on aryl-modified *o*-carboranes, dual emission consisting of LE and CT emission was already observed. By incorporating dual *o*-carborane substituents, solid-state excimer emission can be introduced as the third emission species. It should be emphasized that dual emission properties consisting of excimer and CT emission or LE and CT emission can be selected by choosing the preparation protocol, that is, the type of solvent for recrystallization. Moreover, characteristic thermochromic luminescent behaviors were obtained originating from intensity ratio changes between each emission species. Our findings might be applicable not only to establish precise temperature measurement technologies based on ratiometric analyses but also to design advanced luminochromic materials having high environmental sensitivity. Further investigations on fundamental optical properties of structural variations and solid-state stimuli responsiveness are now in progress in our laboratory.

Acknowledgements

This work was partially supported by the Nakatani Foundation (for K.T.) and JSPS KAKENHI Grant Numbers JP21H02001 and JP21K19002 (for K.T).

References

1. S. K. Behera, S. Y. Park and J. Gierschner, Dual Emission: Classes, Mechanisms, and Conditions, *Angew. Chem. Int. Ed.*, 2021, **60**, 22624–22638.
2. K. Wang, Y. Z. Shi, C. J. Zheng, W. Liu, K. Liang, X. Li, M. Zhang, H. Lin, S. L. Tao, C. S. Lee, X. M. Ou and X. H. Zhang, Control of Dual Conformations: Developing Thermally Activated Delayed Fluorescence Emitters for Highly Efficient Single-Emitter White Organic Light-Emitting Diodes, *ACS Appl. Mater. Interfaces*, 2018, **10**, 31515–31525.
3. R. Gui, H. Jin, X. Bu, Y. Fu, Z. Wang and Q. Liu, Recent advances in dual-emission ratiometric fluorescence probes for chemo/biosensing and bioimaging of biomarkers, *Coord. Chem. Rev.*, 2019, **383**, 82–103.
4. A. S. Klymchenko, Solvatochromic and Fluorogenic Dyes as Environment-Sensitive Probes: Design and Biological Applications, *Acc. Chem. Res.*, 2017, **50**, 366–375.
5. H. L. Lee, H. J. Jang and J. Y. Lee, Single molecule white emission by intra- and inter-molecular charge transfer, *J. Mater. Chem. C*, 2020, **8**, 10302–10308.
6. E. J. McLaurin, L. R. Bradshaw and D. R. Gamelin, Dual-Emitting Nanoscale Temperature Sensors, *Chem. Mater.*, 2013, **25**, 1283–1292.
7. M. A. H. Alamiry, A. C. Benniston, G. Copley, A. Harriman and D. Howgego, Intramolecular excimer formation for covalently linked boron dipyrromethene dyes, *J.*

Phys. Chem. A, 2011, **115**, 12111–12119.

8. H. Yeo, K. Tanaka and Y. Chujo, Synthesis of dual-emissive polymers based on ineffective energy transfer through cardo fluorene-containing conjugated polymers, *Polymer*, 2015, **60**, 228–233.

9. K. Zhang, H. Zhou, Q. Mei, S. Wang, G. Guan, R. Liu, J. Zhang and Z. Zhang, Instant Visual Detection of Trinitrotoluene Particulates on Various Surfaces by Ratiometric Fluorescence of Dual-Emission Quantum Dots Hybrid, *J. Am. Chem. Soc*, 2011, **133**, 8424–8427.

10. Y. Dong, J. Cai, Q. Fang, X. You and Y. Chi, Dual-Emission of Lanthanide Metal-Organic Frameworks Encapsulating Carbon-Based Dots for Ratiometric Detection of Water in Organic Solvents, *Anal. Chem.*, 2016, **88**, 1748–1752.

11. H. Naito, K. Nishino, Y. Morisaki, K. Tanaka and Y. Chujo, Highly-efficient solid-state emissions of anthracene-: *o*-carborane dyads with various substituents and their thermochromic luminescence properties, *J. Mater. Chem. C*, 2017, **5**, 10047–10054.

12. K. Nishino, K. Tanaka, Y. Morisaki and Y. Chujo, Design of Thermochromic Luminescence without Conformation and Morphology Changes by Employing the Bis(*o*-carborane)-Substituted Benzobithiophene Structure, *Chem. Asian J.*, 2019, **14**, 789−795.

13. K. Nishino, K. Uemura, K. Tanaka, Y. Morisaki, and Y. Chujo, Modulation of the *cis*- and *trans*-Conformations in the Bis-*o*-carborane Substituted Benzodithiophenes and Emission Enhancement Effect on Luminescent Efficiency by Solidification, *Eur. J. Org. Chem*., 2018, **2018**, 1507−1512.

14. H. Naito, K. Nishino, Y. Morisaki, K. Tanaka and Y. Chujo, Luminescence Color tuning of Stable Luminescent Solid Materials from Blue to NIR Based on Bis-*o*-Carborane-Substituted Oligoacenes, *Chem. Asian J*., 2017, **12**, 2134−2138.

15. H. Naito, Y. Morisaki and Y. Chujo, *o*-Carborane-based anthracene: A variety of emission behaviors, *Angew. Chem. Int. Ed.*, 2015, **54**, 5084–5087, DOI:10.1002/anie.201500129.

16. K. Nishino, H. Yamamoto, K. Tanaka and Y. Chujo, Development of Solid-State Emissive Materials Based on Multifunctional o-Carborane-Pyrene Dyads, *Org. Lett.*, 2016, **18**, 4064–4067.

17. H. Mori, K. Nishino, K. Wada, Y. Morisaki, K. Tanaka and Y. Chujo, Modulation of luminescence chromic behaviors and environment-responsive intensity changes by substituents in bis-o-carborane-substituted conjugated molecules, *Mater. Chem. Front.*, 2018, **2**, 573–579.

18. K. Kokado and Y. Chujo, Emission via aggregation of alternating polymers with o-carborane and p-phenylene-ethynylene sequences, *Macromolecules*, 2009, **42**, 1418–

1420.

19. J. Ochi, K. Tanaka and Y. Chujo, Recent Progress in the Development of Solid-State Luminescent o-Carboranes with Stimuli Responsivity, *Angew. Chem. Int. Ed.*, 2020, **59**, 9841–9855.

20. K. Nishino, H. Yamamoto, K. Tanaka and Y. Chujo, Solid-State Thermochromic Luminescence through Twisted Intramolecular Charge Transfer and Excimer Formation of a Carborane−Pyrene Dyad with an Ethynyl Spacer, *Asian J. Org. Chem.*, 2017, **6**, 1818–1822.

21. M. Gon, K. Tanaka and Y. Chujo, Recent progress in the development of advanced element-block materials, *Polym. J.*, 2018, **50**, 109–126.

22. S. Ito, M. Gon, K. Tanaka and Y. Chujo, Molecular Design and Applications of Luminescent Materials Composed of Group 13 Elements with an Aggregation-Induced Emission Property, *Natl. Sci. Rev.*, 2021, **8**, nwab049.

23. M. Gon, K. Tanaka and Y. Chujo, Concept of Excitation-Driven Boron Complexes and Their Applications for Functional Luminescent Materials, *Bull. Chem. Soc. Jpn*., 2019, **92**, 7−18.

24. Y. Chujo and K. Tanaka, New Polymeric Materials Based on Element-Blocks, *Bull. Chem. Soc. Jpn*., 2015, **88**, 633−643.

25. H. Naito, K. Nishino, Y. Morisaki, K. Tanaka and Y. Chujo, Solid-State Emission of the Anthracene-o-Carborane Dyad from the Twisted-Intramolecular Charge Transfer in the Crystalline State, *Angew. Chem. Int. Ed.*, 2017, **56**, 254–259.

26. J. Ochi, K. Tanaka and Y. Chujo, Experimental Proofs for Emission Annihilation through Bond Elongation at the Carbon–Carbon Bond in *o*-Carborane with Fused Biphenyl-Substituted Compounds, *Dalton Trans*., 2021, **50**, 1025–1033.

27. K. Nishino, K. Uemura, K. Tanaka and Y. Chujo, Dual emission: Via remote control of molecular rotation of o -carborane in the excited state by the distant substituents in tolane-modified dyads, *New J. Chem.*, 2018, **42**, 4210–4214.

28. J. Ochi, K. Tanaka and Y. Chujo, Improvement of Solid-State Excimer Emission of the Aryl–Ethynyl-o-Carborane Skeleton by Acridine Introduction, *European J. Org. Chem.*, 2019, **2019**, 2984–2988.

29. J. Ochi, K. Tanaka and Y. Chujo, Dimerization-Induced Solid-State Excimer Emission Showing Consecutive Thermochromic Luminescence Based on Acridine-Modified o-Carboranes, *Inorg. Chem.*, 2021, **60**, 8990–8997.

30. K. Nishino, H. Yamamoto, K. Tanaka and Y. Chujo, Time-Dependent Emission Enhancement of the Etynylpyrene-o-Carborane Dyad and Its Application as a Luminescent Color Sensor for Evaluating Water Contents in Organic Solvents, *Chem. Asian J*., 2019, **14**,

1577−1581.

31. K. Wada, K. Hashimoto, J. Ochi, K. Tanaka and Y. Chujo, Rational Design for Thermochromic Luminescence in Amorphous Polystyrene Films with the Bis-*o*-carborane-substituted Enhanced-Conjugated Molecule Having Aggregation-Induced Luminochromism, *Aggregate*, 2021, **2**, e93.

32. H. Yamamoto, J. Ochi, K. Yuhara, K. Tanaka and Y. Chujo, Switching between intramolecular charge transfer and excimer emissions in solids based on aryl-modified ethynyl–o-carboranes, *Cell Reports Phys. Sci.*, 2022, **3**, 100758.

33. J. Ochi, K. Yuhara, K. Tanaka and Y. Chujo, Controlling the Dual-Emission Character of Aryl-Modified o-Carboranes by Intramolecular CH···O Interaction Sites, *Chem. – A Eur. J.*, DOI:10.1002/chem.202200155.

34. K. Nishino, K. Tanaka and Y. Chujo, Tuning of Sensitivity in Thermochromic Luminescence by Regulating Molecular Rotation Based on Triphenylamine-Substituted o-Carboranes, *Asian J. Org. Chem.*, 2019, **8**, 2228–2232.

35. S. Suzuki, S. Sasaki, A. S. Sairi, R. Iwai, B. Z. Tang and G. ichi Konishi, Principles of Aggregation-Induced Emission: Design of Deactivation Pathways for Advanced AIEgens and Applications *Angew. Chem. Int. Ed.*, 2020, **59**, 9856–9867.

36. S. Kim, J. H. Lee, H. So, M. Kim, M. S. Mun, H. Hwang, M. H. Park and K. M. Lee,

Insights into the effects of substitution position on the photophysics of mono-: O -carborane-substituted pyrenes, *Inorg. Chem. Front.*, 2020, **7**, 2949–2959.

37. S. Kim, J. H. Lee, H. So, J. Ryu, J. Lee, H. Hwang, Y. Kim, M. H. Park and K. M. Lee, Spirobifluorene-Based o-Carboranyl Compounds: Insights into the Rotational Effect of Carborane Cages on Photoluminescence, *Chem. - A Eur. J.*, 2020, **26**, 548–557.
38. T. L. Heying, J. W. Ager, S. L. Clark, D. J. Mangold, H. L. Goldstein, M. Hillman, R. J. Polak and J. W. Szymanski, A New Series of Organoboranes. I. Carboranes from the Reaction of Decaborane with Acetylenic Compounds, *Inorg. Chem.*, 1963, **2**, 1089–1092.
39. P. Van Der Sluis and A. L. Spek, BYPASS: an effective method for the refinement of crystal structures containing disordered solvent regions, *Acta Crystallogr. Sect. A*, 1990, **46**, 194–201.
40. M. Montalti, A. Credi, L. Prodi and M. T. Gandolfi *Handbook of Photochemistry third edition* Boca Raton: CRC Press, 2006.

Figure and Tables

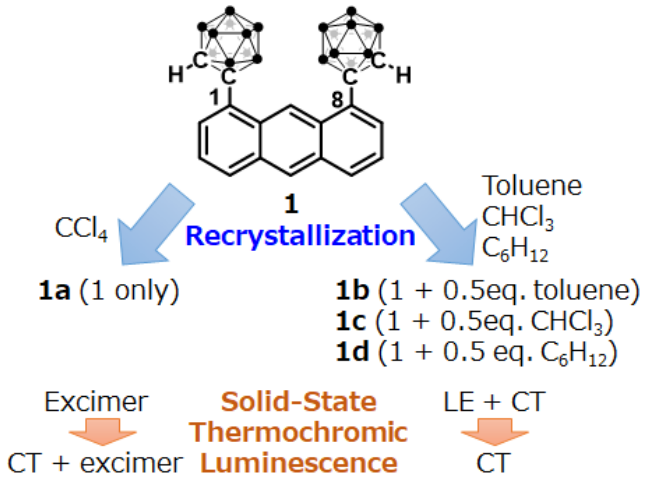

Figure 1. Chemical structure of **1** and schematic illustration for the preparation of crystal polymorphs and their dual-emission properties.

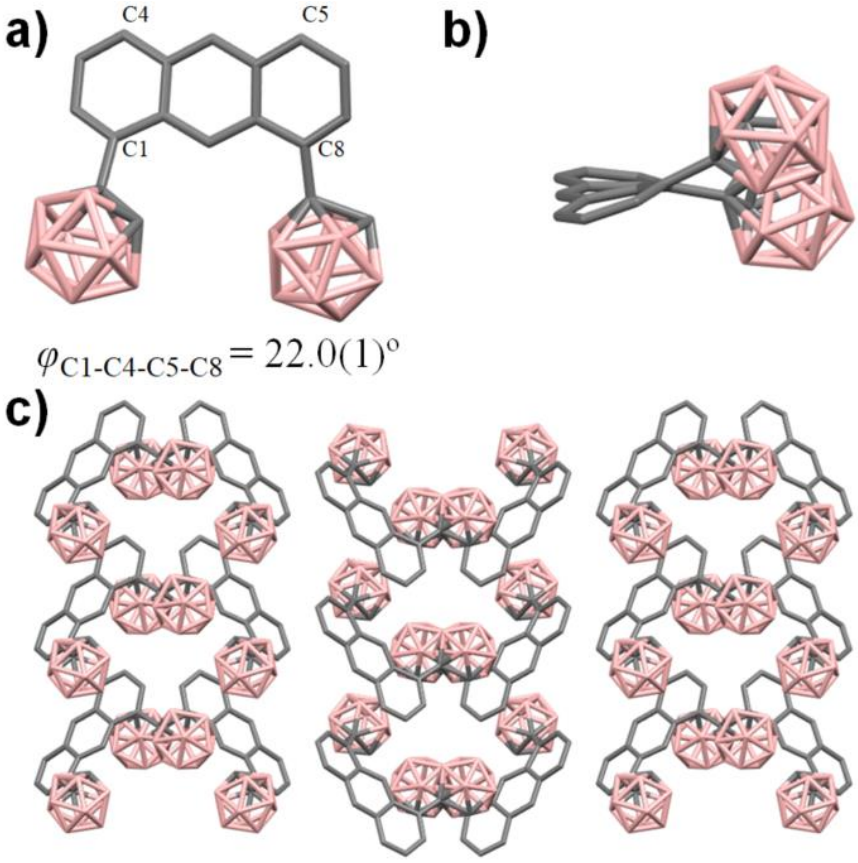

Figure 2. Crystal Structure of **1b**. a) Top and b) side views of molecular structure. c) Packing structure.

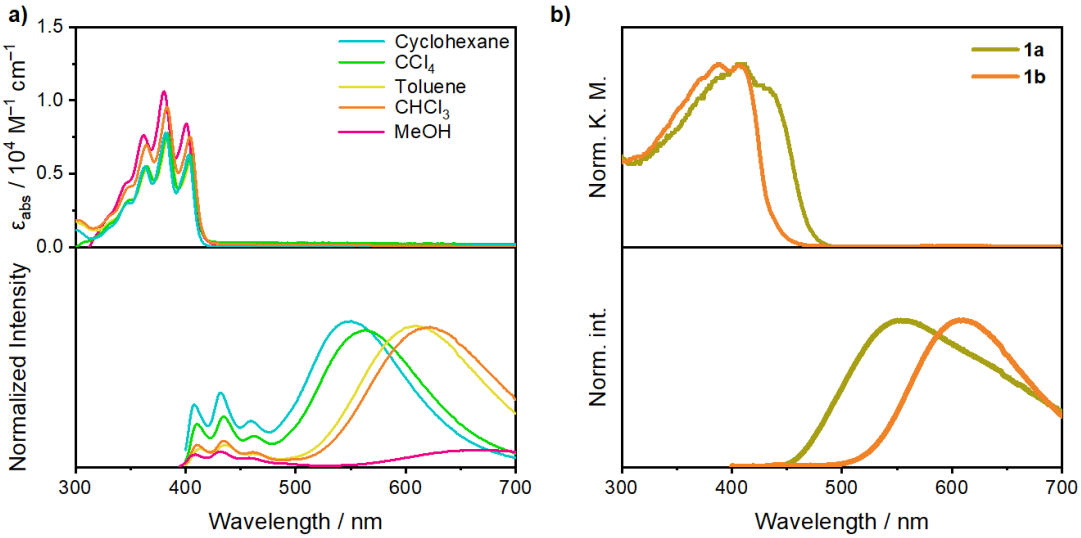

Figure 3. a) UV-Vis absorption (top) and PL spectra (bottom) of **1** in various solvents (1.0×10^{-5} M). b) diffusion reflectance (top) and PL (bottom) spectra of **1a** and **1b**.

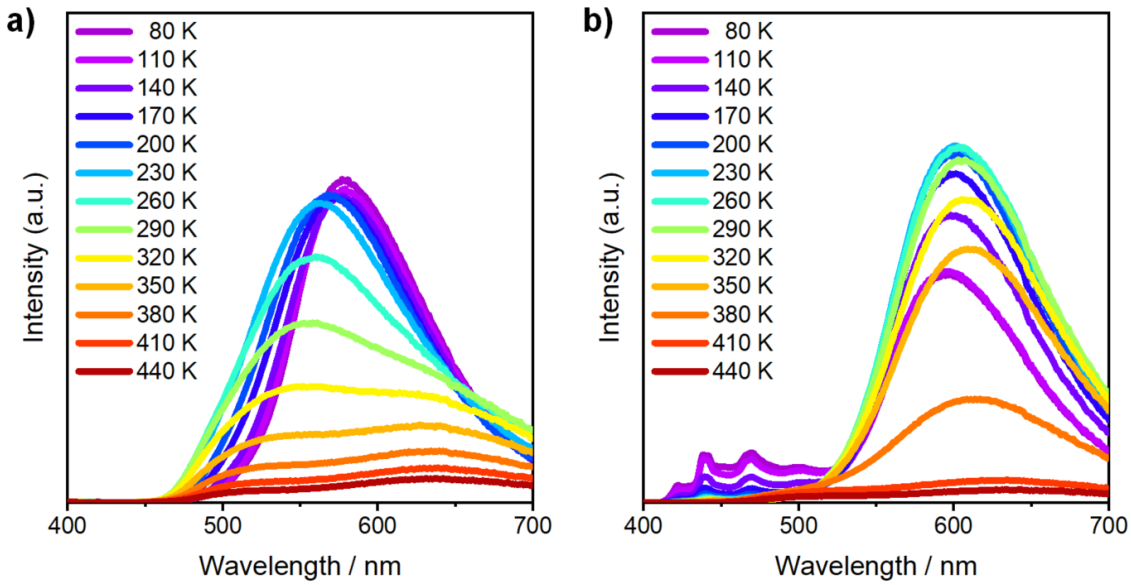

Figure 4. VT-PL spectra of a) **1a** and b) **1b** by heating from 80 K to 440 K.

Table 1. Photophysical properties of **1**

Sample	$\lambda_{PL,max}$ / nm	τ / ns[a,b]	Φ
1($CHCl_3$)	435[c]	n.d.[e]	0.33[c]
	622[c]	9.0	
1a	553[d]	53 (89%), 16 (11%)	0.23[d]
1b	608[d]	11	0.69[d]

[a]Excited at 369 nm.

[b]Detected at $\lambda_{PL,max}$.

[c]Excited at 383 nm.

[d]Excited at 382 nm.

[e]n.d. = not determined due to weak photoluminescence

TOC

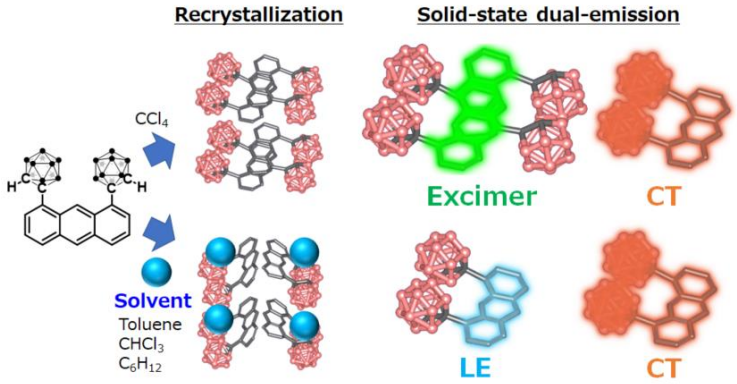
Recrystallization
Solid-state dual-emission
CCl4
Solvent
Toluene
CHCl3
C6H12
Excimer
CT
LE
CT